of Convective Heat Transfer, Springer-Verlag, New York, 1984, pp. 386–428.

[5]Cebeci, T., "Calculation of Unsteady Two-Dimensional Laminar and Turbulent Boundary Layers with Fluctuations in External Velocity." *Proceedings of the Royal Society of London, Series A,* Vol. A355, 1977, pp. 225–238.

[6]Isaacson, E. and Keller, H. B., *Analysis of Numerical Methods,* Wiley, New York, 1966.

Structural Modification to Glass-Like Materials Under Laser Irradiation

D. E. Hastings*
Physical Sciences Inc.
Andover, Massachusetts

I. Introduction

THE scientific questions raised by the coupling of laser radiation into material surfaces have been studied for several years.[1] For glass and glass-like materials there are several mechanisms for laser-induced changes to the material. One of them is bubble formation and growth inside the material while it is softened under the thermal energy deposited by the laser.[2]

For glass-like materials such a fused silica, there is very little dissolved gas, so that bubble growth by absorption of gas cannot be expected to occur. However, there are inhomogeneous quartz materials that are constructed by compressing fibers of quartz together at high temperature and pressure. This process leaves many voids in the material which contain trapped gas. These voids can serve as nucleation sites for bubble growth by expansion of the trapped gas under the laser irradiation. This process of growth will lead to irreversible changes in the glass-like material if the trapped gas is initially "frozen in" out of equilibrium. In this Note we shall address this issue of bubble growth in a glass-like material and the concomitant changes in bulk properties of the material.

II. Bubble Growth for a Single Bubble

We consider a spherical bubble of initial radius R_o containing trapped gas in a glass-like material whose viscosity is $\mu(T)$ where T is the time-varying temperature of the glass around the bubble. The boundary of the bubble $[R(t)]$ grows according to the Rayleigh equation[2,3]

$$R\ddot{R} + \frac{3}{2}\dot{R}^2 = \frac{1}{\rho_1}\left[p_o\left(\frac{T(t)}{T_o}\right)\left(\frac{R_o}{R}\right)^3 - \frac{2\sigma}{R} - 4\mu[T(t)]\frac{\dot{R}}{R}\right] \quad (1)$$

In Eq. (1), $\dot{R} = dR/dt$, ρ_1 is the (liquid) glass density, p_o is the pressure of the trapped gas at temperature T_o and σ is the surface tension of the bubble. In writing Eq. (1) the external pressure has been neglected. This can be justified either by noting that the laser glass interaction may occur in a vacuum or by noting that for the expected pressures in the bubbles ($p_o \gg 1$ atm) an external pressure of up to 1 atm will be small. Also in Eq. (1) the heat from the glass is taken to flow into the bubble sufficiently fast that the gas temperature in the bubble adiabatically follows the glass temperature. For SiO_2 we take the viscosity coefficient as $\mu(T) = \eta_o e^{Q/T}$ where $Q = 30{,}000$ K and $\eta_o = 10^{-3}$ kg-m/s. The surface tension is taken as $\sigma = 0.3$ Nt/m. The Rayleigh equation must be solved subject to the initial conditions $R(0) = R_o$, $\dot{R}(0) = 0$.

The Rayleigh equation was solved numerically by separating Eq. (1) into two first-order equations in time and integrating the coupled set.[4] The temperature of the glass around the bubble will be a function of time as the glass absorbs the laser radiation. In order to be definite, the temperature dependence on time was taken as that given by solving the unsteady one-dimensional energy balance equation for SiO_2 absorbing DF laser radiation.[5] In Fig. 1 a plot of time against bubble radius obtained by solving Eq. (1) is shown for a range of different initial radii. The initial pressure inside the bubble was taken as 5 atm at 300 K. This is a reasonable choice based on the manufacturing process for these materials. Figure 1 indicates that the bubbles did not start growing until after a delay time and then quickly went to their equilibrium radii. The delay in the bubble growth occurs because, below a certain temperature, which we shall call the freezing temperature, the glass is so viscous that no motion of the bubble boundary is possible on the timescale of a few seconds that we are considering. Above this temperature, the glass viscosity decays very rapidly. This freezing temperature is $\simeq 1500$ K. The final bubble radii are based upon the pressure of the trapped gas at $\simeq 1500$ K ($\simeq 25$ atm).

Therefore, from these numerical results, we can deduce that there is a freezing pressure, p_{freeze}, (which is a function of timescale) given approximately by (for a timescale of a few seconds) $p_{\text{freeze}} = p_o(1500/T_o)$. For this freezing pressure the equilibrium solution of Eq. (1) is R_{eq} given by

$$\frac{R_{\text{eq}}}{R_o} = \left(\frac{p_{\text{freeze}} R_o}{2\sigma}\right)^{1/2} \quad (2)$$

Physically, the freezing pressure is the pressure at the freezing temperature above which the glass can flow freely.

III. Equilibrium Bubble Distribution Function

The results of Sec. II show that a set bubble with pressure p_o at T_o in SiO_2 will reach its equilibrium radius given by Eq. (2) during the laser pulse. For a glass-like material of initial volume V_i we define a distribution function for the bubbles by letting $g(R,t)\,dR$ be the number of bubbles at time t with radii between R and $R + dR$. The number of bubbles at any time is then

$$N = \int_0^\infty g(R,t)\,dR \quad (3)$$

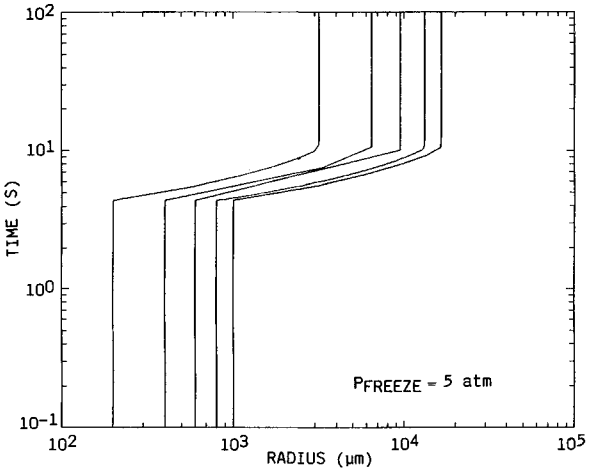

Fig. 1 Time against bubble radius (μm) for the surface temperature profile of a DF 10 s laser pulse in SiO_2.

Received June 28, 1988; revision received Nov. 8, 1988.

*Consultant, Department of Aeronautics and Astronautics, Massachusetts Institute of Technology. Member AIAA.

the average bubble size is

$$\bar{R} = \frac{1}{N}\int_0^\infty Rg(R,t)\,dR \tag{4}$$

and, if the bubbles are all spherical, the porosity of the material whose volume is $V(t)$ is

$$\Theta = \frac{1}{V(t)}\int_0^\infty g(R,t)\,\frac{4}{3}\,\pi R_3\,dR \tag{5}$$

Since we expect that the bubbles will grow until they reach equilibrium and then stop, we shall concentrate on relationships between the initial state and final state of the bubbles and materials and not follow the detailed behavior in time.

We start with conservation of mass for the glass. This gives

$$V_f(1-\Theta_f) = V_i(1-\Theta_i) \tag{6}$$

where subscript i implies initial and subscript f implies final. The volume inside the bubbles is $V_b = V\Theta$, and using Eq. (6) we can obtain

$$\Theta_f = 1 - \frac{1}{1 + (V_{b_f}/V_{b_i})\Theta_i/(1-\Theta_i)} \tag{7}$$

If the laser spot on the material has area A_{spot} and heats to a depth L_i where bubble growth can occur (L_i will be determined by the requirement that $T > 1500$ K), then the surface of the material will "foam" or rise to a height ΔL. From Eq. (7) and using $V_i = A_{\text{spot}}\,L_i$, $V_f = A_{\text{spot}}\,(L_i + \Delta L)$, we obtain

$$\frac{\Delta L}{L_i} = \frac{\Theta_f - \Theta_i}{1-\Theta_i} \tag{8}$$

In writing Eq. (8) we assume that the only motion allowed to the material is for the surface to rise. This is based on the idea that the viscosity of the glass is so high that only glass directly heated by the laser will be able to flow and, therefore, outside of the laser spot area the glass is constrained. If the surface can freely rise then a reasonable physical assumption is that the bubbles grow and do not interact or coalesce since they can move out of each other's way. With this assumption we can write

$$g(R_f)\,dR_f = g(R_i)\,dR_i \tag{9}$$

This expresses conservation of the bubbles and is conceptually equivalent to the Lagrangian form of the equation of conservation of mass in fluid dynamics. From Eqs. (9) and (3) we can see that $N_f = N_i$. We shall require that the initial distribution function have the physical property that for $R_i = 0$ there are no bubbles and for $R_i \to \infty$ there are no bubbles. There properties are reasonable choices based on the manufacturing process where the material is formed by compressing crossed fibers of quartz at high pressure and temperature. This motivates us to choose a model form for $g(R_i)$ as

$$g(R_i) = \frac{4}{\sqrt{\pi}}\,\frac{N_i}{R_s}\left(\frac{R_i}{R_s}\right)^2 e^{-(R_i/R_s)^2} \tag{10}$$

where R_s is some scale radius. This distribution function is chosen because it gives physically reasonable limits for $R_i \to 0$ and $R_i \to \infty$, and it is analytically tractable. The actual distribution function of bubbles must be determined experimentally. We anticipate that for integral properties such as the porosity, results obtained with this hypothetical form should have the correct scalings, although specific numbers will depend on the details of this distribution function.

The scale radius R_s can be related to the initial porosity by use of Eqs. (10) and (5) and in terms of Θ_i and initial bubble density ($\rho_i = N_i/V_i$)

$$R_s = \left(\frac{\Theta_i}{\rho_i}\,\frac{3}{16\sqrt{\pi}}\right)^{1/3} \tag{11}$$

The initial average bubble radius is $\bar{R}_i = 2R_s/\sqrt{\pi}$, while the initial volume contained in the bubbles is

$$V_{b_i} = N_i[(4/3)\pi\bar{R}_i^3](\pi/2)$$

The relationship in Eq. (2) enables us to evaluate the metric in Eq. (9) and obtain the final state in terms of the initial state. We obtain

$$\frac{V_{b_f}}{V_{b_i}} = \frac{105}{32}\sqrt{\pi}\left(\frac{p_{\text{freeze}}\,R_s}{2\sigma}\right)^{3/2} \tag{12}$$

In the high internal pressure limit ($p_{\text{freeze}}\,R_s/2\sigma \gg 1$), we can examine the rise in the surface and show from Eqs. (8) and (12) that

$$\frac{\Delta L}{L_i} \simeq \frac{105}{32}\sqrt{\pi}\left(\frac{3}{15\sqrt{\pi}}\right)^{1/2}\left(\frac{p_{\text{freeze}}\,\Theta_i}{2\sigma}\right)^{3/2}\frac{1}{\rho_i^{1/2}}$$

IV. Discussion and Conclusions

In Fig. 2 we show a plot of $\Delta L/L_i$ against p_{freeze} for two values of the initial porosity. In both cases the curves indicate a power law dependence on the pressure. We find that we are in the high pressure limit because the initial bubble density chosen ($\rho_i = 10^{15}$ m^{-3}) is such that the initial mean bubble radius is only a few microns. This is consistent with the fact that the mean separation between bubble centers is 10 μm. We see that fairly large values of the fractional change in surface height can be obtained. For a typical DF pulse, we might have $L_i \simeq 0.25$ cm so that a rise of surface height of 0.35 cm at p_{freeze}

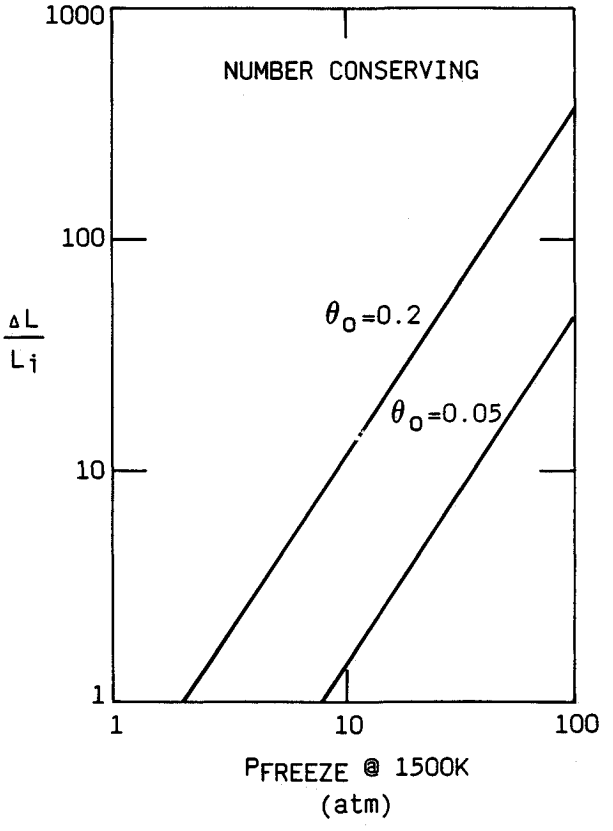

Fig. 2 Fractional change in height of surface against p_{freeze} in atmosphere for two initial values of the porosity, $\sigma = 0.3$ Nt/m, $\rho_i = 10^{15}$ m^{-3}.

of 10 atm and with $\Theta_i = 5\%$ would be expected. The final porosity for this case is in excess of 40%.

This theoretical treatment of this laser material interaction could be tested by measuring the distribution function in a sample of material made from quartz fibers and then measuring macroscopic quantities like porosity after laser irradiation. The foaming of the surface of the material can also be measured and used to deduce the frozen-in pressure in the bubbles.

Acknowledgments

The author would like to thank Dr. Peter Nebolsine for suggesting this problem to him. Useful discussions were also held with Dr. Alan Gelb. Norman Hummer kindly provided the temperature-time profiles, while Gary Snyder performed many of the numerical computations.

References

[1]Ready, J. F., *Effects of High-Power Laser Radiation*, Academic Press, New York, 1971.

[2]Hastings, D. E., "Bubble Growth in Laser Irradiated Glass," *Journal of Applied Physics*, Vol. 54, 1983, pp. 2223-2229.

[3]Plesset, M. A. and Prosperetti, A., *Annual Review of Fluid Mechanics*, Vol. 9, 1977, pp. 145-185.

[4]Shampine, L. F. and Gordon, M. K., *Computer Solution of Ordinary Differential Equations: The Initial Value Problem*, W. H. Freeman, San Francisco, 1975.

[5]Bloemberger, N., "Report to the American Physical Society of the Study Group on Science and Technology of Directed Energy Weapons," *Review of Modern Physics*, Vol. 59, No. 3, Part II, 1987, pp. 1-202.

Experimental Results for the Quasisteady Heat Transfer Through Periodically Contacting Surfaces

W. M. Moses*
Texas A&M University, College Station, Texas
and
R. R. Johnson†
North Carolina State University, Raleigh, North Carolina

Introduction

QUASISTEADY-STATE heat transfer across two surfaces coming into regular, periodic contact has been examined analytically by Howard and Sutton[1] and Mikhailov[2] under the assumption of perfect thermal contact at the interface. Howard and Sutton[3] and Vick and Ozisik[4] have extended this analysis to include the effects of thermal contact resistance at the contact interface, with Howard[5] undertaking an additional experimental study. Moses and Johnson[6] experimentally examined the behavior of thermal contact resistance during the quasisteady state and the time required to approach the quasisteady-state condition. This paper experimentally examines the influence of the cycle contact and separation times and the thermal contact conductance on the quasi-steady-state temperature distribution across periodically contacting surfaces.

Presented as Paper 87-1608 at the AIAA 22nd Thermophysics Conference, Honolulu, HI, June 8-10, 1987; received May 17, 1988; revision received Jan. 22, 1988.

*Assistant Professor, Department of Mechanical Engineering. Member AIAA.

†Associate Professor, Department of Mechanical and Aerospace Engineering.

Experimental Apparatus

The mathematical model of the experimental problem is the same as that considered by Vick and Ozisik[4] for finding the temperature distribution, $T(x,t)$, for one-dimensional heat transfer through two specimens with thermal conductivity, k, and thermal diffusivity, α, each of length L, heated at $x = 0$ and cooled at $x = 2L$, with the contact interface at $x = L$. The experimental apparatus (detailed by Moses and Johnson[6,7]) consists of two test cylinders—each held at one end in a thermal reservoir, the supporting frame, and the equipment required to bring the test specimens uniformly into and out of contact. The contact mechanism consists of two main plates. A thermal reservoir is suspended below the upper plate, with an alignment ball and a spring-loaded alignment mechanism to maintain the proper alignment of the test surfaces. The second thermal reservoir is attached to the lower plate, which slides along the four PVC rods forming the supporting frame. This plate is made of Teflon to reduce binding in the sliding contact. The specimens are caused to contact and separate by driving the lower plate with a pneumatic cylinder.

The test specimens are 0.0254 m in diameter and 0.1397 m in total length. On each cylinder 0.0381 m on one end is threaded to fit into the fluid reservoir. Copper-constantan thermocouples are located on the centerline of each specimen at 0.0127-m intervals for the 0.0508 m adjacent to the contact surface. Two additional copper-constantan thermocouples are on the specimen centerline—0.005 and 0.1011 m from the contact surface. The lateral surface of the test specimens is insulated with a Teflon sleeve, cut for thermocouple access and to allow the thermocouples to move freely in a vertical direction as the surfaces move into and out of contact. Separate experiments indicate that the heat flow in the test specimens is one-dimensional.[7] Thermal properties and surface characteristics of the test specimens are listed in Table 1. The test specimens are nominally flat and free of coatings or surface oxidation.

Procedure and Data Acquisition

After the test specimens come to steady state while separated, the timer is activated to start the experiment. To reduce the number of variables influencing the thermal contact conductance, the air-pressure regulator is set to provide an applied load at the contact interface of 85-90 kPa and the mean temperature of the interface at the end of the contact interval is kept at 33°C. Temperature measurements are made at 10-s intervals.

The temperature distribution is available directly from the experimental output. The thermal contact conductance, h_c, is computed from the apparent temperature drop, ΔT, and the heat flux, q'', across the interface, according to the definition $h_c = q''/\Delta T$. The apparent temperature drop across the interface is obtained with a least-squares quadratic regression to curve fit independently the experimental data from each test specimen. The heat flux at the contact interface is computed from Fourier's law using the least-squares curve fit of the temperature distribution. The overall uncertainty for these experiments is 21% for aluminum, 14% for brass, and 11% for copper.[7]

Table 1 Properties and surface roughness of test specimens

Specimen type/designation	k, W/mC	$\alpha \times 10^5$, m^2/s	Length, m	Roughness, CLA, μm
Aluminum 1	167.2	6.7	0.1016	5.207
Aluminum 2	167.2	6.7	0.1016	4.750
Brass 3	106.1	3.4	0.1016	0.439
Brass 4	106.1	3.4	0.1016	0.635
Copper 1	385.4	9.5	0.1016	2.134
Copper 2	385.4	9.5	0.1016	2.413